

Experimental Study on Reinforcement of Subgrade Slope with Loess-based Grout and Composite Soil Nails

Long Zhao^{1,a}, Shuaihua Ye^{*,2,3,b}, Yilei Shi^{1,c}, Liangliang Xin^{2,3,d}

¹Gansu CSCEC Municipal Engineering Investigation And Design Institute Co., Ltd., Lanzhou, Gansu 730000, China.

²Key Laboratory of Disaster Mitigation in Civil Engineering of Gansu Province, Lanzhou University of Technology, Lanzhou 730050, China;

³Western Center of Disaster Mitigation in Civil Engineering, Ministry of Education, Lanzhou University of Technology, Lanzhou, 730050, China.

^a120083299@qq.com, ^byeshuaihua@163.com

^c1321781334@qq.com, ^dliangliangxin2022@163.com

Abstract: In order to investigate the impact of controllable low-strength yellow soil slurry as grouting material and slope protection layer on the stability and bearing capacity of roadbed slopes. The study used yellow soil as the main experimental material, combined with additives such as cement, sodium sulfate, and ethylene glycol, successfully developing a controllable low-strength fluid material, namely, yellow soil slurry. Based on this, with steel bars as reinforcing material and yellow soil slurry as grouting material and slope protection layer, indoor scaled model tests were conducted relying on the similarity principle, using the yellow soil from a roadbed slope project in Lanzhou. Using slope top settlement and foot bulge as mechanical response indicators, the study investigated the effects of slope gradient, soil nail length, angle, and spacing on the stability and bearing capacity of roadbed slopes. Experimental results indicate that indoor model tests found that the gentler the slope, the higher the stability, and soil nail length and density can enhance the bearing capacity of the roadbed; the reinforcement effect on the roadbed slope is most significant when the angle between the soil nail and the horizontal direction is around 10°. The study results are of reference significance for the application of yellow soil slurry in roadbed slope engineering.

Keywords: Slope engineering; Loess-based Grout; Soil nails; Roadbed bearing capacity; Model experiments.

1. Introduction

The northwest region of China has a unique topography with numerous high embankment slopes. As a crucial part of China's infrastructure, highways play a vital role in the national economy. Many high embankment slopes in the face of various environmental factors such as natural weathering and rainfall erosion have long grappled with severe stability and bearing capacity issues. In practical engineering, the stability of embankment slopes often directly affects the safe operation and lifespan of highways. Traditional reinforcement methods, such as concrete slope protection and geogrids, have drawbacks, including large engineering quantities, long construction periods, and high costs. Therefore, exploring an efficient, economical, and environmentally friendly technique for reinforcing loess-based embankment slopes is crucial for improving construction practices and enhancing the quality of roadbed projects. This has significant implications for the service life of highways and the conservation of social resources in the northwest region.

Currently, numerous scholars have conducted extensive research on the preparation of low-strength flowable fill materials [1-4]. The research mainly focuses on the selection of materials, mix ratio design, analysis of mechanical properties and microscopic mechanisms, the impact of additives on material characteristics, and engineering applications [5-8]. Low-strength flowable fill materials have a wide range of applications, including the backfilling of tunnels and building deep foundation pits in construction and municipal engineering, as well as backfilling in mining engineering for mined-out areas and bridge abutments in highway engineering [9-10]. Loess-based

grout is a type of controllable low-strength flowable construction material. With the promotion of the "dual-carbon" strategy, there is a growing demand in the construction field for green and low-carbon materials. In this context, loess-based grout, as a controllable low-strength novel material, has attracted significant attention due to its strong flowability, simple preparation, and low carbon emissions. Loess-based grout primarily utilizes loess as the main material, incorporates inorganic non-metallic material cement as a solidifying agent, and, with the addition of specific additives, enhances the performance of the solidified loess-based grout [11-12].

In road embankment engineering, the stability and bearing capacity of slopes have always been a focal point of attention [13-14]. Therefore, an in-depth study of the mechanical effects of loess-based grout in the reinforcement of road embankment slopes not only contributes to the material's practical application but also provides new insights and technical means for the design and construction of highway infrastructure [15]. This paper uses steel bars as reinforcing materials, employs loess-based grout as injection material and slope protection surface, and forms loess-based grout composite soil nails to reinforce road embankment slopes, presenting a novel solution to the stability issues of road embankment slopes. The research utilizes loess from Lanzhou as the experimental material, incorporating cement, sodium sulfate, and ethylene glycol as additives, successfully developing a controllable low-strength flowable material. Building on the developed loess-based grout, relying on a road embankment slope project in Lanzhou, indoor reduced-scale model tests were conducted. The study investigates the influence of slope gradient, soil nail length, soil nail angle, and soil nail spacing on the bearing capacity and stability of road embankment slopes when loess-based grout is used as the injection material for composite soil nails. Through this research, the widespread application of loess-based grout in the field of road embankment reinforcement can be promoted.

2. Indoor Model Test

Based on the developed loess-based grout, using it as the injection material and slope protection surface, with steel bars as reinforcing elements, forming loess-based grout soil nails. Taking a road embankment slope project in Lanzhou as an example, indoor reduced-scale model tests were conducted based on the similarity theory. Loading was applied on the loading plate to study the influence of slope gradient, soil nail length, angle, and density on the top settlement and toe uplift. The effects of loess-based grout composite soil nails on the stability and bearing capacity of road embankment slopes were explored. Figure 1 shows the on-site image of the road embankment slope, and Figure 2 displays the model box.



Fig.1 Field Testing of Road Embankment Slopes

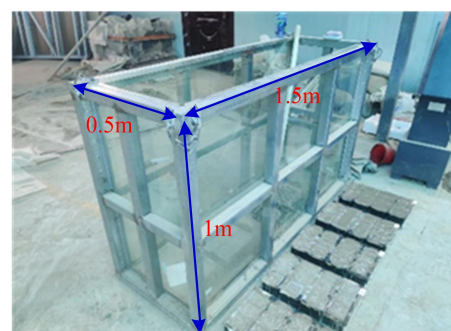


Fig.2 Model Box

2.1 Experimental Materials and Equipment

Calculate the weight of each layered fill soil based on compaction density, layer filling, and compaction. Loess parameters are detailed in Table 1.

Table 5 Basic Physical Mechanical Parameters of loess Samples

Bulk Density (kN/m ³)	Internal Friction Angle (°)	Cohesion (kPa)	Poisson's Ratio	Deformation Modulus (MPa)
17.8	30	23	0.3	20.0

(1) Sieving: Dry soil preparation involves natural drying of the test soil, crushing, sieving through a 0.5 mm mesh, and finally, the sieved soil is sealed for preservation. (2) Mixing: Calculate the required mass of soil based on the volume of the model box, spread the soil evenly on a waterproof cloth, spray a measured amount of water evenly using an electric sprayer, and then mix the soil. (3) Compaction: Wrap the soil completely with a waterproof cloth, seal it, and leave it undisturbed for 7 days.

2.2 Galvanized Iron Wire

Replace steel bars with galvanized iron wire, and the mechanical parameters are listed in Table 2.

Table 6 Model Reinforcement Parameters

Property	Diameter (mm)	Area (mm ²)	Yield Strength (MPa)
Galvanized Wire	1.8	2.54	360

2.3 Support Materials

Both the grouting and spray surface materials utilize loess-based grout, with various parameters detailed in Table 7.

Table 3 Support Material Parameters

Material	Cement Mixing Ratio (%)	Moisture Content (%)	Age (d)
Soil Nail Grout	18	35	14
Spray Surface	18	35	7

3. Experimental Design

3.1 Layout of Measurement Points

Following the reference [16], monitoring points are arranged at the slope's crest and toe to measure settlement and uplift values. At a distance of 2 cm from the slope surface at the crest, a 1 cm × 1 cm iron piece is horizontally placed as a monitoring point for crest settlement displacement. At a distance of 2 cm from the slope surface at the bottom, a 1 cm × 1 cm iron piece is horizontally placed as a monitoring point for toe uplift displacement. Displacement is measured using a dial gauge. Two 2 cm × 2 cm wooden bars are horizontally placed on the slope surface, with a small steel plate fixed in the middle. The magnetic dial seat attaches to the steel plate, and then the dial gauge is installed on the magnetic dial seat and kept level. Adjust the magnetic dial seat to position the dial gauge at the center of the iron piece. See Figure 3 for the layout of monitoring points.

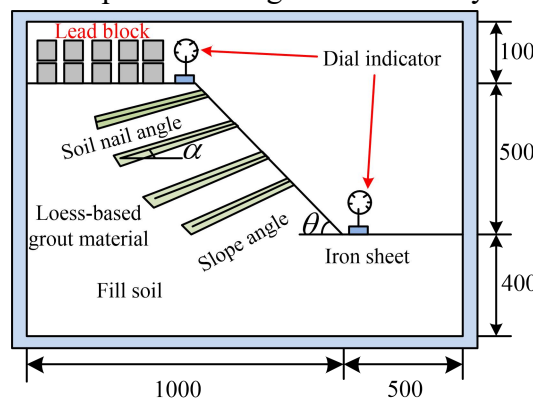


Fig.3 Layout Schematic of Monitoring Points

3.2 Experimental Condition Design

To investigate the effects of slope gradient, soil nail length, angle, and density on the stability and bearing capacity of the embankment slope, an orthogonal experimental design method was employed. The experimental conditions are outlined in Table 4. The standard model had a slope gradient of 1:0.5, soil nail length of 0.5 m, an angle of 10° with the horizontal plane, and a spacing of 0.15 m. Following the principle of controlling variables, models for the remaining conditions were prepared and tested. See Table 4 for the experimental conditions.

Table 4 Experimental Condition Parameters

Experimental Scheme	Slope Gradient θ	Soil Nail Length L	Soil Nail Angle α	Soil Nail Spacing k
Different control groups	1:0.5	0.2m	0°	0.1m
	1:0.67	0.3 m	10°	0.15m
	1:1	0.4 m	20°	0.2
	-	0.5 m	-	-

3.3 Experimental Steps and Loading Conditions

The model test adopts layered filling, with soil filling and compaction from bottom to top in 9 layers, each layer having a thickness of 10 cm. The compaction coefficient is controlled at 0.9. After the soil filling is completed, the slope is cut to the design slope with a blade, and finally, holes are manually drilled.

Steel wires with a diameter of 2 mm are placed in the holes, and then loess-based cement grout is injected to form loess-based cement grout composite soil nails. Finally, a 0.8 mm steel wire mesh is fixed on the slope surface, and loess-based cement grout is sprayed and leveled. The loading is carried out step by step by stacking lead blocks on the slope top, starting from 10 kPa and increasing by 10 kPa per level. Readings are taken after each level of loading. The stability criterion is determined by considering the settlement, and if the settlement is less than 0.1 mm per hour for two consecutive hours, it is deemed stable, and the next level of load is applied. The experimental process is shown in Figure 4.

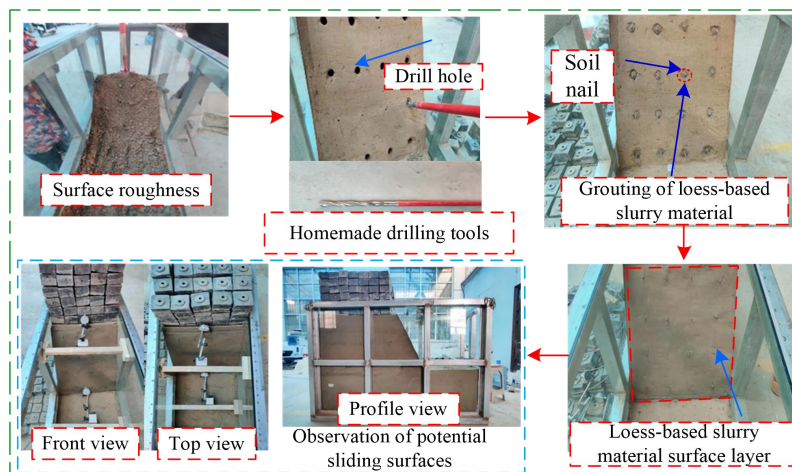


Fig.4 Model Fabrication and Loading Process

4. Experimental Data Analysis

4.1 Influence of Slope Gradient on Stability and Bearing Capacity

(1) Influence of Loess-based Grout Composite Soil Nails on the Bearing Capacity of the Road Embankment Slope

Slope gradient is 1:0.5, nail length is 0.5 m, the angle between the nail and the horizontal direction is 10°, and the spacing is 0.15 m. The influence of soil nails on the stability and bearing capacity of the slope is shown in Figure 5. As depicted in Figure 5, in the model without soil nails, with the increase of the load on the slope top, uplift occurs at the slope foot, and downward displacement occurs at the slope top. When the slope fails, the ultimate bearing capacity is 210 kPa, slope top settlement is 6.5 mm, and slope foot uplift is 1.8 mm. After adding soil nails, the ultimate bearing capacity is 260 kPa, slope top settlement is 5 mm, and slope foot uplift is 2.2 mm. Compared with the slope without soil nails, adding soil nails increases the ultimate bearing capacity of the road embankment slope by 50 kPa, a 24% improvement, reduces slope top settlement by 1.5 mm, but increases slope foot uplift by 0.4 mm. This indicates that the composite soil nails formed by loess-based grout and steel reinforcement increase the shear strength of the soil when subjected to forces on the slope top, enhancing the ability to restrain soil deformation. Therefore, soil nails have a positive effect on improving the stability and bearing capacity of the slope.

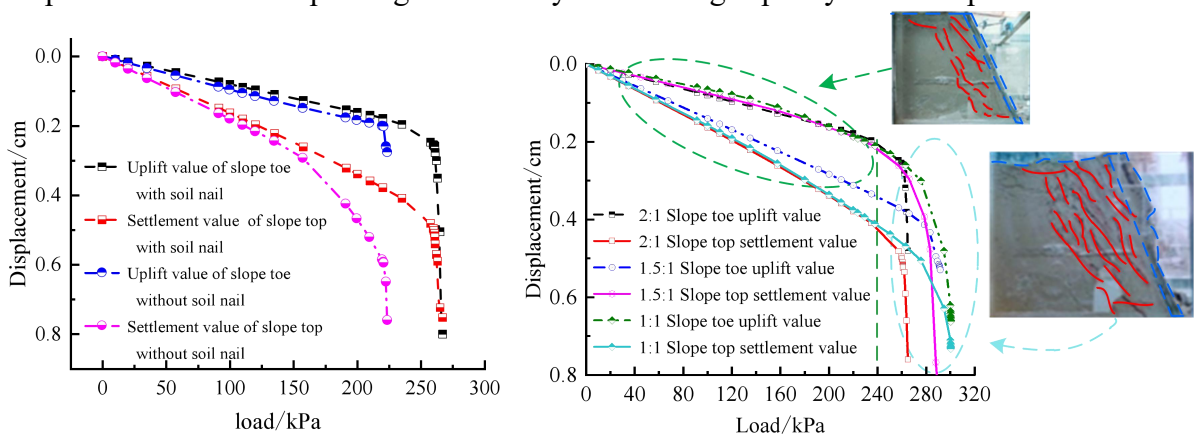


Fig.5 Influence of Soil Nails on Slope Deformation at the Same Slope Angle

Fig.6 Influence of Composite Soil Nails on Slope Deformation Response with Varying Slopes

(2) Influence of Slope Gradient on Stability and Bearing Capacity

Slope gradients of 2:1, 1.5:1, and 1:1 is considered, with a nail length of 0.5 m, an angle of 10° with the horizontal direction, and a spacing of 0.15 m. The impact of slope gradient on the stability and bearing capacity of the slope is shown in Figure 6. As illustrated in Figure 6, when the slope top load is relatively small, the load-displacement curve shows a linear relationship. As the load increases, the sliding surface does not penetrate. When the load increases to between 240 kPa and 300 kPa, the load-displacement relationship exhibits obvious nonlinearity, and cracks appear in the interior of the slope model. When the sliding surface completely penetrates, reaching the ultimate bearing capacity, the slope fails.

4.2 Influence of Nail Length on Stability and Bearing Capacity

Nail lengths of 0.2 m, 0.3 m, 0.4 m, and 0.5 m were considered, with a slope gradient of 1:0.5, a nail angle of 10° with the horizontal direction, and a spacing of 0.15 m. The impact of nail length on the slope foot uplift and slope top settlement is shown in Figures 7 and 8, respectively.

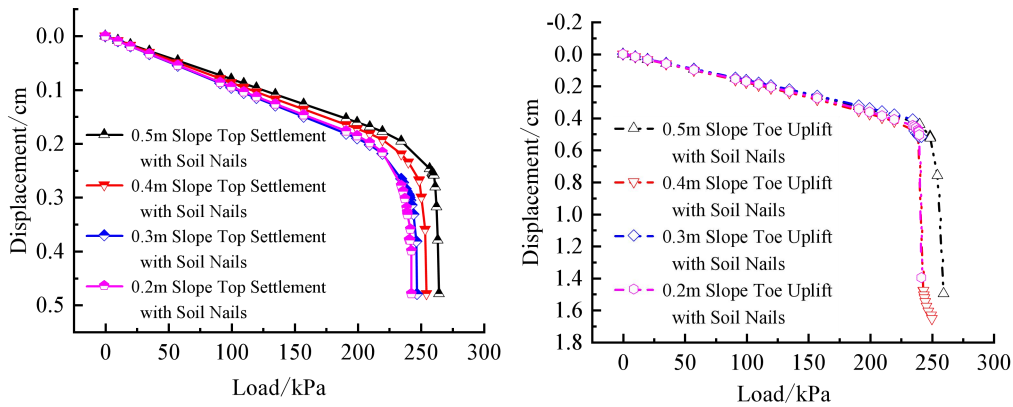


Fig.7 Influence of Soil Nail Length on Slope Top Displacement
 Fig.8 Influence of Soil Nail Length on Slope Foot Displacement

From Figures 7 and 8, it can be observed that when the nail length is 0.2 m and 0.3 m, the load-displacement relationship of the slope is similar, and the ultimate bearing capacity of the slope remains relatively constant at 230 kPa. The reason for this is that when the slope nail is shallow, the sliding surface forms behind the nail, and the entire slope, including the nail, slides downward, resulting in lower stability and bearing capacity. As the nail length increases, the nail penetrates through the potential sliding surface, and the sliding surface at the nail exhibits a stepwise pattern. The presence of the nail enhances the shear resistance of the soil, leading to an increase in bearing capacity.

4.3 Effect of Nail Angle on Stability and Bearing Capacity

The angles between the nail and the horizontal direction are 0°, 10°, and 20°, with a slope inclination of 1:0.5, nail length of 0.5 m, and spacing of 0.15 m. The impact of the nail angle on the slope's top settlement and foot uplift is shown in Figures 9 and 10.

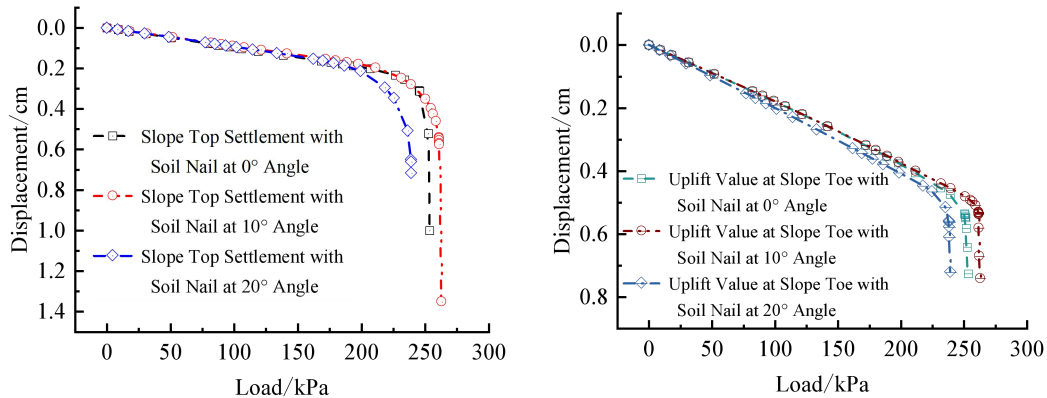


Fig.9 Influence of Soil Nail Angle on Slope Top Displacement
 Fig.10 Influence of Soil Nail Angle on Slope Foot Displacement

From Figures 9 and 10, it can be observed that the ultimate bearing capacity of the slope is 250 kPa, 260 kPa, and 240 kPa for nail angles of 0°, 10°, and 20°, respectively. It is evident that the slope's ultimate bearing capacity is highest when the nail angle is 10°. Therefore, the nail angle plays a crucial role in determining the slope's ultimate bearing capacity, with an optimal insertion angle of approximately 10°.

4.4 Effect of Nail Density on Stability and Bearing Capacity

Nail spacing is set at 0.1 m, 0.15 m, and 0.2 m, with a slope inclination of 1:0.5, nail length of 0.5 m, and a nail angle of 10°. The impact of nail density on the slope's top settlement and foot uplift is shown in Figures 11 and 12.

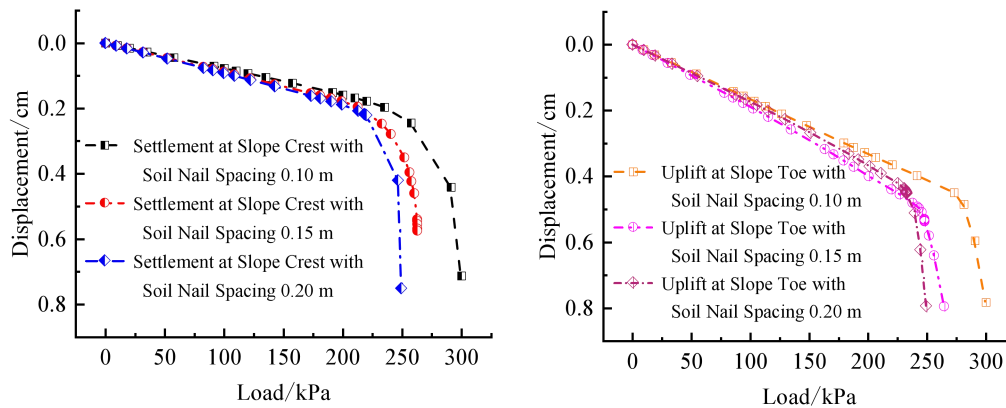


Fig.11 Influence of Soil Nail Density on Slope Top Displacement
 Fig.12 Influence of Soil Nail Density on Slope Foot Displacement

From Figures 11 and 12, it is evident that nail density significantly affects the slope's ultimate bearing capacity. As nail density increases, the ultimate bearing capacity of the slope improves. The ultimate bearing capacities for nail spacings of 0.1 m, 0.15 m, and 0.20 m are 300 kPa, 260 kPa, and 250 kPa, respectively. The higher nail density enhances the restraint capability on the soil, resulting in increased bearing capacity. The sliding surface has difficulty penetrating areas with higher nail density, exhibiting a sawtooth shape at the nail locations. In contrast, lower nail density allows the sliding surface to gradually transition from a sawtooth shape to a circular arc shape.

5. Conclusion

This study, using loess as the primary material and cement, additives, etc., as auxiliary materials, conducted indoor model tests on the influence of loess-based composite soil nails on the stability and bearing capacity of road embankment slopes. Based on a road embankment slope project in Lanzhou, the following conclusions were drawn:

(1) The gentler the slope inclination, the higher the stability. When the slope ratio is 1:1, the road embankment's bearing capacity increases by approximately 25% compared to a slope ratio of 1:0.5. The length of the soil nails has a negligible impact on the road embankment's bearing capacity unless the soil nail length is long enough to embed into the stable soil behind the sliding surface, effectively limiting the formation of the sliding surface and inhibiting its development.

(2) There is an optimal angle for the insertion of soil nails into the soil. Model tests indicate that an angle of around 10° is optimal. The loess-based grout material bonds with the surrounding soil, resisting radial tension and enhancing the road embankment's resistance to shear forces, thereby increasing the embankment's bearing capacity. Higher soil nail density results in greater restrictions on the sliding of the road embankment, leading to an increased bearing capacity.

Acknowledgements

Gansu Provincial Natural Science Foundation(2020-0405-JCC-1768); Gansu Province key research and development Program(23YFGA0083).

References

- [1] YI F, GUAN M, LI J, et al. Mechanical properties and mechanism analyses of rice husk ash geopolymer solidified soil[J]. *Hydrogeology & Engineering Geology*, 2022, 49(2): 94-101.
- [2] PHUMMIPHAN I, HORPIBULSUK S, RACHAN R, et al. High calcium fly ash geopolymer stabilized lateritic soil and granulated blast furnace slag blends as a pavement base material[J]. *Journal of Hazardous Materials*, 2018, 341: 257 – 267

- [3] YU J, CHEN Y, CHEN G, et al. Mechanical behaviour of geopolymer stabilized clay and its mechanism[J]. *Journal of Building Materials*, 2020, 23 (2) : 364 – 371.
- [4] JIA D, PEI X, ZHANG X, et al. A test study of the microscopic mechanism of modified glutinous rice mortar solidified loess[J]. *Hydrogeology & Engineering Geology*, 2019, 46 (6) : 90 – 96
- [5] ZHOU H, WANG X, HU X, et al. Influencing factors and mechanism analysis of strength development of geopolymer stabilized sludge[J]. *Rock and Soil Mechanics*, 2021, 42 (8) : 2089 – 2098
- [6] DENG Y, WU Z, LIU S, et al. Influence of geopolymer on strength of cement-stabilized soils and its mechanism[J]. *Chinese Journal of Geotechnical Engineering*, 2016, 38 (3) : 446 – 453
- [7] YE H, ZHANG W, WEI W, et al. Experimental study on the curing of soft soil with activator-geopolymer[J]. *Journal of Basic Science and Engineering*, 2019, 27 (4) : 906 – 917.
- [8] GHADIR P, RANJBAR N. Clayey soil stabilization using geopolymer and Portland cement[J]. *Construction and Building Materials*, 2018, 188: 361 – 371.
- [9] ZHOU Y X, WANG J Z. Principle of ready-mixed solidified soil and its prospects for engineering application[J]. *New Building Materials*, 2019, 46(10):117-120.
- [10] KIM Y S, DO T M, KIM H K, et al. Utilization of excavated soil in coal ash-based controlled low strength material (CLSM) [J] .*Construction and Building Materials*, 2016, 124: 598-605.
- [11] Liu Dongrui. Experimental Study on Cemented Soil Flowable Fill Materials in Loess Region [D]. Lanzhou University of Technology, 2023.
- [12] Li Yaxi, Wang Qin, Zhang Qiuchen et al. Effect of inorganic curing agent on structure and properties of convection-cured soil [J]. *Materials Review*, 2023, 37(S1):156-162
- [13] Wang Yicheng. Application research of fluid-solidified soil in subgrade Engineering [D]. Jilin University, 2021.
- [14] Guo Zhiming. Application of cement improved expansive soil in subgrade Engineering [J]. *Building Technology*, 2023, 54(15):1875-1879.
- [15] Gao Zichen. Study on road performance of ready-mixed fluidcured soil [D]. Chang 'an University, 2023.
- [16] SONG Ye. Experimental Study on the Assembled Flexible Surface Soil Nailing Wall Support Structure System [D]. Beijing University of Civil Engineering and Architecture, 2022.